Approaching total absorption at near infrared in a large area monolayer graphene by critical coupling

Yonghao Liu, Arvinder Chadha, Deyin Zhao, Jessica R. Piper, Yichen Jia, Yichen Shuai, Laxmy Menon, Hongjun Yang, Zhenqiang Ma, Shanhui Fan, Fengnian Xia, and Weidong Zhou

---

Approaching total absorption at near infrared in a large area monolayer graphene by critical coupling

Yonghao Liu,[1] Arvinder Chadha,[1] Deyin Zhao,[1] Jessica R. Piper,[2] Yichen Jia,[3] Yichen Shuai,[1] Laxmy Menon,[1] Hongjun Yang,[1] Zhenqiang Ma,[4] Shanhui Fan,[2] Fengnian Xia,[3] and Weidong Zhou[1,a)]

[1]Nanophotonics Lab, Department of Electrical Engineering, University of Texas at Arlington, Arlington, Texas 76019, USA
[2]Ginzton Laboratory, Department of Electrical Engineering, Stanford University, Stanford, California 94305, USA
[3]Department of Electrical Engineering, Yale University, New Haven, Connecticut 06520, USA
[4]Department of Electrical and Computer Engineering, University of Wisconsin-Madison, Madison, Wisconsin 53706, USA

We demonstrate experimentally close to total absorption in monolayer graphene based on critical coupling with guided resonances in transfer printed photonic crystal Fano resonance filters at near infrared. Measured peak absorptions of 35% and 85% were obtained from cavity coupled monolayer graphene for the structures without and with back reflectors, respectively. These measured values agree very well with the theoretical values predicted with the coupled mode theory based critical coupling design. Such strong light-matter interactions can lead to extremely compact and high performance photonic devices based on large area monolayer graphene and other two–dimensional materials. © 2014 AIP Publishing LLC. [http://dx.doi.org/10.1063/1.4901181]

Over the past decade, the unique electronic and optical properties of graphene have generated strong interests in developing optoelectronic and electronic devices based on graphene and other layered two–dimensional material.[1–6] However, the nature of ultra-thin monolayer structure limits their optical properties on light absorption and emission. A suspended atomically thin layer ($\sim$0.34 nm thickness) of intrinsic graphene exhibits absorption of 2.3% in the infrared to visible spectral range for surface-normal vertically incident light.[7] The weak optical absorption of monolayer graphene limits its photoresponsivity for graphene-based photodetectors.[8,9] Increasing the light-matter interactions in graphene is highly desirable for high-performance graphene-based optical devices.

Enhancement of graphene absorption up to 100% (total absorption) has been investigated in both the visible and infrared spectral ranges.[10] At mid- and far-infrared, graphene exhibits a strong plasmonic response, where enhanced absorption can be achieved via patterned graphene structures, or coupling unpatterned graphene layer with metallic or dielectric grating structures. At shorter optical wavelengths (visible and near-infrared, with wavelength $\lambda < 2 \mu m$), the plasmonic resonance is absent for undoped, unpatterned graphene. Enhanced absorption in graphene at near infrared has been proposed by placing graphene inside various micro- and nano-cavities, such as integrating graphene with silicon photonic waveguide,[11] photonic crystal line defect cavities,[12] plasmonic nanostructures,[13,14] and other photonic structures.[15–18]

Recently, Piper and Fan proposed a *total* absorption scheme in the optical regime by coupling unpatterned monolayer graphene with patterned defect-free photonic crystal slab (PCS) via critical coupling with guided resonance.[10] The out-of-the-plane optical mode coupling is feasible with the Fano or guided resonance effect associated with defect-free PCS, where these in-plane guided resonances above the light-line (leaky mode) are also strongly coupled to the out-of-the-plane radiation modes due to phase matching provided by the periodic PCS lattice structure. Based on coupled mode theory, total absorption in graphene has been theoretically demonstrated by critical coupling to a guided resonance of a PCS with a back reflector, either a lossless metallic mirror or a realistic multilayer dielectric mirror, in the visible and near-infrared regime.[10] Additionally, the authors also proposed and investigated another generalized total absorption scheme via degenerate critical coupling.[19] In this case, total absorption can be also achieved even without a back reflector.

In this paper, we report experimental demonstrations of the critically coupled total absorption from monolayer graphene at 1550 nm near-infrared wavelength range, based on two step transfer printing process to form the desired multilayer stacking structure on a transparent glass substrate. As shown schematically in Fig. 1(a), the structure considered here consists of a monolayer graphene transferred onto a silicon PCS on a glass substrate. For a symmetric two-port system supporting a single resonance, the theoretical maximum of absorption due to the resonance is 50%.[10] For the system, since the index contrast between silica below the silicon layer and air above the silicon layer is sufficiently small, such that as a simple approximation one can consider this to be a symmetric structure. To achieve total (100%) absorption, a perfect back (metal) reflector can be introduced, as shown schematically in Fig. 1(b). Also shown in Figs. 1(c) and 1(d) are scanning electron micrographs (SEM) and micrographs of fabricated device structure on silicon-on-insulator (SOI) and on glass substrate, respectively.

The transmission/reflection spectra of these structures were simulated using the Fourier modal method with
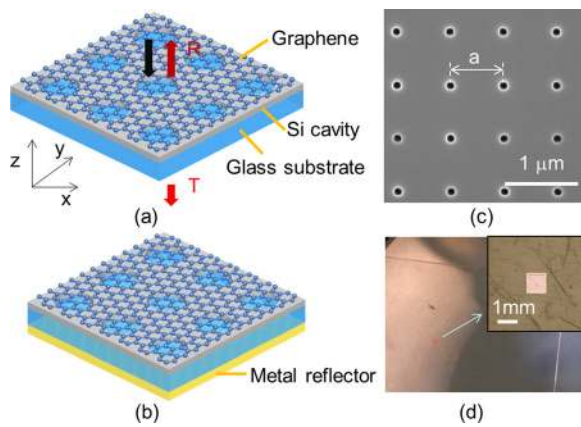
---

a)wzhou@uta.edu

FIG. 1. (a) and (b) Schematics of graphene on Si photonic crystal cavity (a) without and (b) with a back metal reflector; (c) a SEM top view image of the fabricated Si photonic crystal slab on SOI substrate; and (d) a micro-graph of the device under study here with a tri-layer configuration (monolayer graphene/Si photonic crystal slab/glass substrate) via two step transfer printing processes. A zoom-in image shows the patterned Si photonic crystal area completely covered with large area mono-layer graphene.

Stanford Stratified Structure Solver (S^4) software package.[20] We first consider Si PCS on glass structure, without graphene on top. Following similar design procedures reported earlier,[21,22] we consider Si PCS layer thickness of 249 nm and index of 3.48. The square lattice constant (*a*) and air hole radius (*r*) were chosen to have operation wavelength close to 1550 nm spectral band. For the device reported here, *a* = 770 nm and *r/a* = 0.09 (i.e., *r* = 70 nm).

Based on the design parameters, Si PCS Fano resonance filter was first fabricated on a SOI substrate using e-beam lithography (EBL) and reactive-ion etching (RIE) processes.[23] The top view SEM of the fabricated photonic crystal structures on the SOI is shown in Fig. 1(c). After selective-etching the buried oxide of the patterned SOI section with pure hydrofluoric acid, the Si PCS was released (detached from the Si substrate) and transferred onto a glass substrate with Polydimethylsiloxane (PDMS) stamp using transfer

printing process.[22,24,25] Finally, large area monolayer graphene, grown on copper substrate by chemical vapor deposition,[26] was transferred on top of the Si PCS on glass substrate, with a thin spun-on Poly(methyl methacrylate) (PMMA) layer on top as the graphene transfer supporting layer.[27] Shown in Fig. 1(d) is the micrograph of the patterned Si PCS on a glass substrate, completely covered with a large area monolayer graphene. Since PMMA is optically transparent at operation wavelength around 1550 nm, all simulations and measurements are carried out with a thin (180 nm) PMMA layer on top of the monolayer graphene.

Devices were characterized by measuring the surface-normal transmission (T) and reflection (R) spectra with an Agilent tunable laser system (spectral coverage from 1468 nm to 1572 nm) with 10 pm resolution and 9 dBm output power. The incident beam goes through an optical circulator, a laser beam collimator, a glass lens, and a beam splitter. Reflection and transmission spectra were collected with two optical detectors simultaneously, configured and calibrated as part of the Agilent lightwave optical return loss measurement system. The incident beam spot size is ~150 μm in diameter, much smaller than the 1 mm^2 Si PCS pattern area. Care was taken to ensure that the incident beam angle is collimated with surface-normal direction.[22,28] In order to minimize the Fabry-Perot oscillation associated with the finite glass substrate thickness, a drop of index-matching oil was applied to the backside of the glass substrate. Finally, the absorption (A) can be derived based on the equation A = 1-T-R, ignoring very small percentage of other scattering losses.

Shown in Figs. 2(a) and 2(b) are the measured (solid line) and simulated (dashed line) transmission (T) and reflection (R) spectra for the Si PCS Fano filter on glass, without the transferred graphene layer. The resonance occurs at 1537 nm with a Q factor of 2100, estimated by fitting with Fano resonance formula.[29] To establish a baseline/reference on the absorption in the structure, measured absorption (A) spectra for the Si PCS on glass were derived based on A = 1-T-R
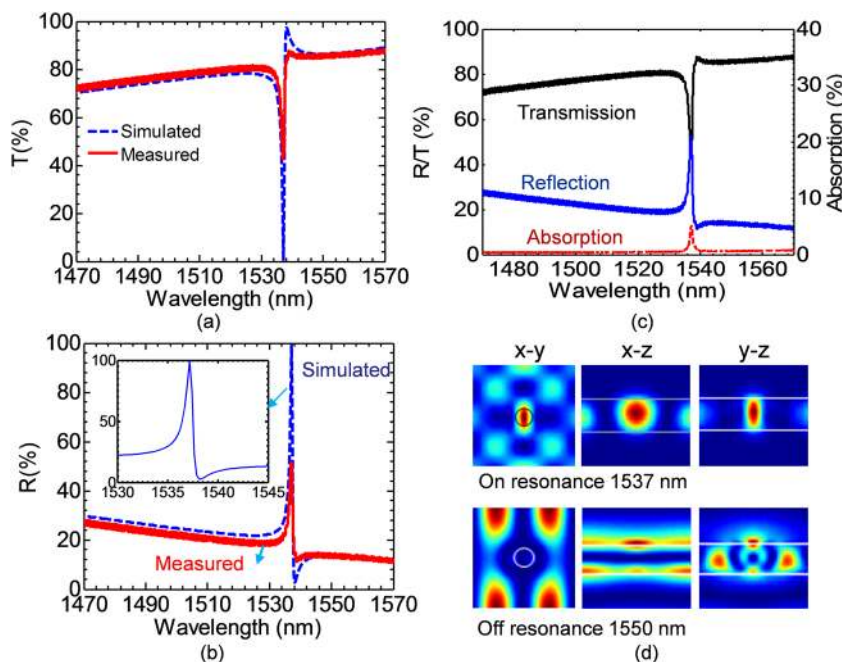

FIG. 2. (a) and (b) Measured and simulated (a) transmission and (b) reflection spectra of Si PCS transferred on glass substrate, with the inset in (b) showing the zoom-in of the simulated reflection resonance; (c) measured transmission and reflection spectra, and derived absorption spectrum for the Si PCS on glass substrate, without graphene layer; and (d) simulated field distributions for on-resonance (1537 nm) and off-resonance (1550 nm) modes, with the x, y, and z coordinates defined in Fig. 1(a).
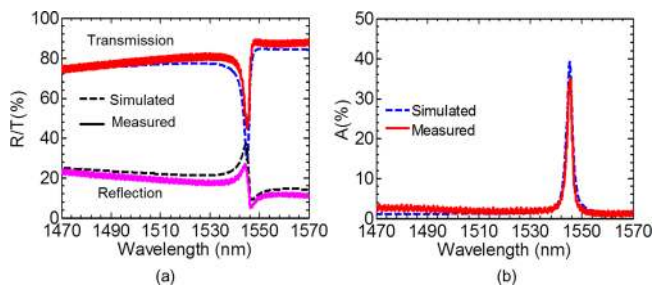
FIG. 3. (a) Measured (solid line) and simulated (dashed line) transmission (T) and reflection (R) spectra for the monolayer graphene on Si PCS without back reflector, as shown in Fig. 1(a); and (b) measured and simulated absorption (A) spectra for the monolayer graphene on Si PCS without back reflector.

with the results shown in Fig. 2(c). Notice in theory that the absorption should be zero as Si is non-absorbing at this wavelength region. However, we do see a 5% absorption peak around resonance. This measurement artifact is largely related to the measurement resolution limit and the impact of the non-ideal surface-normal incident angle.

Resonance modal properties were also investigated. Snapshots of the electrical field $|E|^2$ in plane (x-y cross-sectional plane through the center of the silicon slab) and along cross-sectional planes (x-z and y-z planes) are shown in Fig. 2(d), for on- and off-resonance locations. Well defined confinement mode can be seen for the on-resonance condition.

After transferring monolayer graphene onto the Si PCS, the device was characterized again by measuring transmission and reflection, as shown in Fig. 3(a). Notice that the measured resonant wavelength red-shifted to 1545.5 nm, as a result of increased index on top, with a monolayer graphene and a 180 nm thick PMMA layer. Also shown in Fig. 3(a) are the simulated transmission/reflection spectra for the device under test. For the simulation, the refractive index of PMMA is taken as 1.5 and the absorption is ignored due to

small absorption coefficient around 1500 nm.[30] The graphene thickness is taken as 0.34 nm with the refractive index n = 3 + i5.446λ/3 μm^{-1}.[31] Both simulation and measurement results agree very well.

Following the same procedure, absorption (A) was extracted from the measured and simulated transmission/reflection spectra, as shown in Fig. 3(b). The measured absorption in graphene was enhanced from 2%–3% (off resonance) to 35% (on resonance) due to the presence of Fano filter. Accordingly, the simulated absorption has a maximum absorption of 39% at resonance peak wavelength of 1545.5 nm. This experimental demonstration offers a very encouraging and promising route towards extremely high absorption devices. With the optimized design, it is possible to achieve 50% peak absorption at resonance under critical coupling condition.[10]

To further increase the absorption, a metal reflector (100 nm Au coated glass substrate) was placed to the backside of the 1 mm thick glass substrate. As predicted earlier,[10] it is possible to achieve perfect 100% absorption under critical coupling condition, as the addition of the back reflector changes the system from a two-port system to a one-port system. Since there is no transmission now (T = 0), the absorption can be extracted from the measured reflection spectrum (A = 1-R). Both measured reflection (R) and extracted absorption (A) are shown in Fig. 4(a). The peak absorption increases to ∼85%. Notice that the oscillations on the measured reflection spectrum (and also on the extracted absorption spectrum) are due to the Fabry-Perot oscillations originated from the finite glass substrate thickness (1 mm). To accurately estimate the peak absorption, a best fit of the absorption spectrum was carried out based on Fast Fourier Transform (FFT), shown as the red absorption spectrum line in Fig. 4(a). The original measured absorption signal was filtered by taking a FFT, removing the high frequency Fabry-Perot oscillations, and then using the inverse Fourier transform to reconstruct the absorption signal. Care was taken to
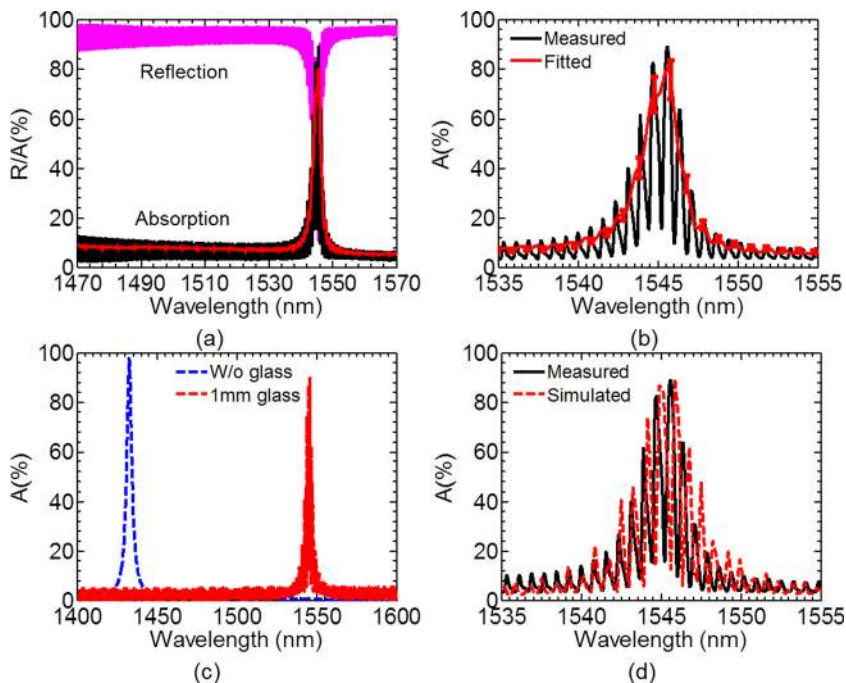

FIG. 4. (a) Measured reflection (R) and absorption (A = 1-R) spectra for graphene on Si PCS with back reflector, as shown schematically in Fig. 1(b). The fitted smooth absorption spectrum (red line) is obtained via FFT process to eliminate the Fabry-Perot oscillations associated with the finite glass substrate thickness. (b) Zoom-in of the measured and fitted absorption spectra near resonance; and (c) simulated absorption spectra for the monolayer graphene on Si PCS cavity with ideal back reflectors separated with 1 mm thick glass substrate. For comparison, the resonance absorption with ideal back reflector is also simulated without glass substrate. And (d) zoom-in of the measured and simulated absorption spectra near resonance with 1 mm glass substrate.

ensure accurate fit around resonance location, with the zoom-in spectra shown in Fig. 4(b). Additional simulations were carried out to simulate the absorption properties for the structure with a perfect reflector on the back. The results are shown in Fig. 4(c), for two cases without and with a 1 mm glass substrate separating the Si PCS and the back reflector. For the case with 1 mm glass substrate separation, the simulated absorption spectrum agrees very well with the measured one, with similar resonance peak location/amplitude and oscillation features, as shown in the zoom-in spectra of Fig. 4(d). It is worth noting that by placing perfect reflector right below the Si PCS structure (i.e., without glass substrate separation), peak absorption close to 100% can be achieved at resonance location, which is blue-shifted to 1432 nm for the design demonstrated here. So it is feasible to achieve 100% absorption by optimizing the device design and structure, by transferring the graphene and silicon Fano filter directly onto a multilayer dielectric Bragg reflector (DBR).

In conclusion, monolayer graphene absorption was measured on a silicon photonic crystal Fano resonance filter transferred on a glass substrate. We experimentally obtained peak absorption of 35% and 85% for cases without and with back reflectors, respectively. The results agree very well with the theoretically estimated values of 39% and 90%, respectively. With optimization in design parameters and device structures, it is feasible to achieve 100% total absorption. The work can lead to a wide range of ultra-compact and high performance photonic and optoelectronic devices, such as high responsivity and high speed graphene detectors, modulators, and light sources.

[1]A. K. Geim and K. S. Novoselov, Nat. Mater. **6**(3), 183 (2007).
[2]F. Bonaccorso, Z. Sun, T. Hasan, and A. Ferrari, Nat. Photonics **4**(9), 611 (2010).
[3]K. Kim, J.-Y. Choi, T. Kim, S.-H. Cho, and H.-J. Chung, Nature **479**(7373), 338 (2011).
[4]Q. Bao and K. P. Loh, ACS Nano **6**(5), 3677 (2012).
[5]A. Grigorenko, M. Polini, and K. Novoselov, Nat. Photonics **6**(11), 749 (2012).
[6]F. Xia, H. Yan, and P. Avouris, Proc. IEEE **101**(7), 1717 (2013).
[7]R. R. Nair, P. Blake, A. N. Grigorenko, K. S. Novoselov, T. J. Booth, T. Stauber, N. M. R. Peres, and A. K. Geim, Science **320**(5881), 1308 (2008).
[8]F. Xia, T. Mueller, Y.-m. Lin, A. Valdes-Garcia, and P. Avouris, Nat. Nanotechnol. **4**(12), 839 (2009).
[9]T. Mueller, F. Xia, and P. Avouris, Nat. Photonics **4**(5), 297 (2010).
[10]J. R. Piper and S. Fan, ACS Photonics **1**(4), 347 (2014).
[11]X. Gan, R.-J. Shiue, Y. Gao, I. Meric, T. F. Heinz, K. Shepard, J. Hone, S. Assefa, and D. Englund, Nat. Photonics **7**(11), 883 (2013).
[12]R.-J. Shiue, X. Gan, Y. Gao, L. Li, X. Yao, A. Szep, D. Walker, Jr., J. Hone, and D. Englund, Appl. Phys. Lett. **103**(24), 241109 (2013).
[13]T. J. Echtermeyer, L. Britnell, P. K. Jasnos, A. Lombardo, R. V. Gorbachev, A. N. Grigorenko, A. K. Geim, A. C. Ferrari, and K. S. Novoselov, Nat. Commun. **2**, 458 (2011).
[14]Y. Liu, R. Cheng, L. Liao, H. Zhou, J. Bai, G. Liu, L. Liu, Y. Huang, and X. Duan, Nat. Commun. **2**, 579 (2011).
[15]X. Gan, K. F. Mak, Y. Gao, Y. You, F. Hatami, J. Hone, T. F. Heinz, and D. Englund, Nano Lett. **12**(11), 5626 (2012).
[16]A. Ferreira, N. M. R. Peres, R. M. Ribeiro, and T. Stauber, Phys. Rev. B **85**(11), 115438 (2012).
[17]M. Furchi, A. Urich, A. Pospischil, G. Lilley, K. Unterrainer, H. Detz, P. Klang, A. M. Andrews, W. Schrenk, G. Strasser, and T. Mueller, Nano Lett. **12**(6), 2773 (2012).
[18]M. G. Rybin, A. S. Pozharov, C. Chevalier, M. Garrigues, C. Seassal, R. Peretti, C. Jamois, P. Viktorovitch, and E. D. Obraztsova, Phys. Status Solidi B **249**(12), 2530 (2012).
[19]J. R. Piper, V. Liu, and S. Fan, Appl. Phys. Lett. **104**(25), 251110 (2014).
[20]V. Liu and S. Fan, Comput. Phys. Commun. **183**(10), 2233 (2012).
[21]Y. Shuai, D. Zhao, Z. Tian, J.-H. Seo, D. V. Plant, Z. Ma, S. Fan, and W. Zhou, Opt. Express **21**(21), 24582 (2013).
[22]W. Zhou, D. Zhao, Y.-C. Shuai, H. Yang, S. Chuwongin, A. Chadha, J.-H. Seo, K. X. Wang, V. Liu, S. Fan, and Z. Ma, Prog. Quantum Electron. **38**(1), 1 (2014).
[23]Y. Shuai, D. Zhao, A. Singh Chadha, J.-H. Seo, H. Yang, S. Fan, Z. Ma, and W. Zhou, Appl. Phys. Lett. **103**(24), 241106 (2013).
[24]M. A. Meitl, Z. T. Zhu, V. Kumar, K. J. Lee, X. Feng, Y. Y. Huang, I. Adesida, R. G. Nuzzo, and J. A. Rogers, Nat. Mater. **5**(1), 33 (2006).
[25]W. Zhou, Z. Ma, H. Yang, Z. Qiang, G. Qin, H. Pang, L. Chen, W. Yang, S. Chuwongin, and D. Zhao, J. Phys. D: Appl. Phys. **42**(23), 234007 (2009).
[26]X. Li, W. Cai, J. An, S. Kim, J. Nah, D. Yang, R. Piner, A. Velamakanni, I. Jung, E. Tutuc, S. K. Banerjee, L. Colombo, and R. S. Ruoff, Science **324**(5932), 1312 (2009).
[27]J. W. Suk, A. Kitt, C. W. Magnuson, Y. Hao, S. Ahmed, J. An, A. K. Swan, B. B. Goldberg, and R. S. Ruoff, ACS Nano **5**(9), 6916 (2011).
[28]A. S. Chadha, D. Zhao, S. Chuwongin, Z. Ma, and W. Zhou, Appl. Phys. Lett. **103**(21), 211107 (2013).
[29]B. Luk'yanchuk, N. I. Zheludev, S. A. Maier, N. J. Halas, P. Nordlander, H. Giessen, and C. T. Chong, Nat. Mater. **9**(9), 707 (2010).
[30]L. A. Eldada, A. Nahata, and J. T. Yardley, Proc. SPIE **3288**, 175 (1998).
[31]M. Bruna and S. Borini, Appl. Phys. Lett. **94**(3), 031901 (2009).